
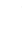






Drill String Vibration Monitoring as an Element of Automatic Control of Drilling

Vladimir Morkun¹^a, Natalia Morkun¹^b, Vitalii Tron²^c, Alona Haponenko³^d,
Iryna Haponenko³^e and Evhen Bobrov³^f

¹Faculty of Engineering Sciences, Bayreuth University, Universitätsstraße, 30, Bayreuth, 95447, Germany

²Department of Automation, Computer Science and Technology, Kryvyi Rih National University,
11 Vitalii Matusevych Str., Kryvyi Rih, 50027, Ukraine

³Research Department, Kryvyi Rih National University,
11 Vitalii Matusevych Str., Kryvyi Rih, 50027, Ukraine

Keywords: Drilling, Vibration, Monitoring, Automatization, Ore, Mining.

Abstract: The research is aimed at monitoring drill string vibrations as an element of automatic control of the drilling process. To reduce negative impacts of vibrations occurring in the drill string at deep drilling of hard rocks, a mathematical model is proposed to consider parameters of the drilling process and predict the penetration rate. The following parameters are used as input variables when studying drilling data: weight-on-bit, rotations per minute, torque, mechanical specific energy, longitudinal, transverse and torsional vibrations. In this study, the rate of penetration is used as a resulting variable. Considering these parameters, a mathematical model of the drilling process is formed on the basis of adaptive neural-fuzzy inference structures. The accuracy of this model is 95.56 %.

1 INTRODUCTION


Deep drilling of hard rocks causes strong vibrations in the drill string associated with a reduced rate of penetration (ROP) and early failure of equipment (Cobern, 2003; Morkun et al., 2015c). The only available method of limiting vibrations during drilling is to change the rotary speed or weight-on-bit (WOB). Yet, these changes often reduce drilling efficiency.


There are a number of vibration sources in a drilling rig that can potentially reduce the mechanical rate of penetration and cause vibrations damaging sensors and clamps. These include, in particular, shock vibrations from bit cones and blades (Morkun et al., 2015c; Golik et al., 2015). There are several cones on the bit which make the string vibrate when moving. Vibration frequency is a multiple of


the speed of the bit blades.


Besides, in drilling there is a direct precession – lateral vibration – caused by imbalance in the drill string (Cobern, 2003; Morkun et al., 2015b). The imbalance can occur due to peculiarities of machining drill collars or due to their curvature, these causing lateral vibrations along the drill string. The reverse precession is caused by friction between the drill string and the borehole. If there is a sufficient contact effort and rotary speed, couplings begin to rotate around the borehole counterclockwise with the frequency that depends on the external diameter of the couplings and that of the borehole. This creates an imbalance effort on the drill string. Excitation is a multiple of the motor speed multiplied by the number of rotor blades.


In addition, the stabilizers have blades in contact with the borehole (Cobern, 2003; Deng et al., 2021). The resulting excitation is a multiple of the rotary speed multiplied by the number of blades. Straight blades cause greater vibration than inclined ones. The stick-slip phenomenon is another source of vibration caused by friction between couplings or stabilizers and the borehole as a result of gravity along the drill


^a <https://orcid.org/0000-0003-1506-9759>

^b <https://orcid.org/0000-0002-1261-1170>

^c <https://orcid.org/0000-0002-6149-5794>

^d <https://orcid.org/0000-0003-1128-5163>

^e <https://orcid.org/0000-0002-0339-4581>

^f <https://orcid.org/0000-0002-9275-3768>

string (Cobern, 2003; Moharrami et al., 2021). This phenomenon can make the element bit jammed. After accumulating enough effort to release the drill string, it resumes its rotation at a high angular speed.

The roller-cone bit is a kind of mechanism that, when interacting with the borehole bottom, converts rotation of the drill string or the borehole motor shaft in longitudinal, torsional, and under certain conditions, transverse vibrations (Novikov and Serikov, 2020; Bogomolov and Serikov, 2018). Strong vibrations during machine operation can cause destruction of drill collars and derrick elements, damage to borehole motors and equipment, an increase in the borehole diameter, early wear of the bit, reduction of the mechanical penetration rate. With intensified vibrations and no control of their level, the phenomenon of resonance can occur, which in most cases results in severe destruction of elements of drill collars and the bit (Bogomolov and Serikov, 2018; Morkun et al., 2015a).

Longitudinal and torsional vibrations are essentially connected with specific design of roller-cone bits and the principle of their operation (Novikov and Serikov, 2020; Liu et al., 2021). Vibrations are of a wavelike nature. They are classified into longitudinal, transverse and torsional. They occur simultaneously and depend on wavelike characteristics of the drill string and devices included in its assembly (calibrators, centrators, dampers, shock absorbers), bit size, properties of drilled rocks, and drilling mode parameters.

The causes of vibrations include a stick-slip nature of rock destruction, rough borehole bottom (Serikov and Ginzburg, 2015; Morkun and Tron, 2014), inhomogeneity, fracturing and sharp intermittency in hardness of drilled rocks, pressure differences under different support teeth of the bit (Novikov and Serikov, 2020; Serikov et al., 2016), uneven wear of teeth leading to formation of different contact areas with the rock; the toothed working surface of the bit, pressure pulsation in the discharge system (Vasiliev et al., 2015; Morkun et al., 2014) and discrete tool feed.

2 MATERIALS AND METHODS

In paper (Sharma et al., 2021) a lumped mass drill rod model that consists of two degrees of freedom was suggested. The drill rod is represented by the equivalent mass and rigidity for axial and torsional motions (figure 1).

Equations of for axial and torsional motions the drill string are as follows:

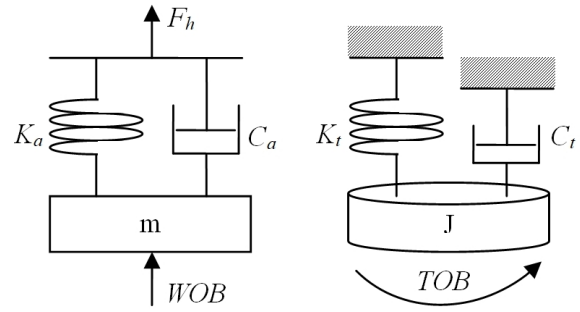


Figure 1: Simplified lumped model for axial and torsional motion: a – axial motion; b – torsional motion (Sharma et al., 2021).

$$m\ddot{x} + c_a\dot{x} + k_a(x - v_0 * t) = -WOB \quad (1)$$

$$J\ddot{\theta} + c_t\dot{\theta} + k_t(\theta - \Omega * t) = -TOB \quad (2)$$

where m is the effective mass of the drill rod, x is the axial displacement, J is the effective polar inertia moment, c_a is the damping coefficient during the axial motion, c_t is the damping coefficient during torsional motion, k_a is the axial rigidity, k_t is the torsional rigidity, v_0 is the initial axial velocity, θ is the angular displacement of the bit and Ω is the surface rotation rate in radians per second (RPS). Axial and torsional motion equations (1) and (2) are related due to interaction forces of the bit.

A method of direct quantitative determination of various vibration forms with parameters that can be easily transmitted to the surface was substantiated in (Cobern, 2003). The system uses four accelerometers and a magnetometer mounted on the drill string. By using various combinations of accelerometer output signals, it is possible to distinguish a whirl, a stick slip, a rebound of the bit, and lateral vibrations from each other. Three accelerometers are mounted in the cuff at the angle of 120 degrees from each other and oriented radially to be measured. The fourth accelerometer is installed axially. The magnetometer is also installed in one of the pockets. The pockets can also accommodate WOB and TOB (time on bottom) strain gauges providing a complete toolkit for borehole diagnostics. Installing accelerometers radially (figure 2) enables direct calculation of various vibration modes.

Radial accelerometers measure the centrifugal force, which is directly related to the rotary speed (Cobern, 2003). As a result, the rotary speed, the stick-slip and the swirl can be directly calculated. The magnetometer is used as a backup for measuring the rotary speed. To measure axial vibration, only a single-axis accelerometer is required. These parameters are calculated as follows.

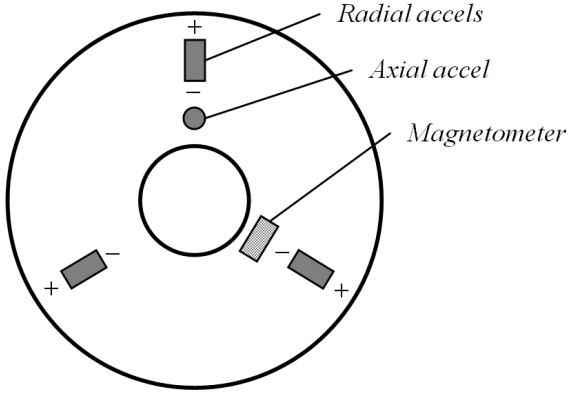


Figure 2: Drill collar sensors.

3 RESULTS AND DISCUSSION

Analysis of frequency characteristics of vibrations during drill string operation indicates different frequency ranges for individual technical components. In particular, Cobern (Cobern, 2003) reveals that vibrations of components cause vibrations of the following frequency: bit rotation – 1000 Hz, stick-slip motion of the bit – 10 Hz, direct precession – 10 Hz, reverse precession – 100 Hz. Also, the vibrations produced by these sources differ significantly in amplitude.

Transfer functions in a closed form associating deformation of the drill string with displacement on the bit in the dimensionless form are described by the following expressions:

$$\frac{\bar{X}_b}{\bar{W}_b}(\bar{s}) = \Psi_a h_a(\bar{s}) = -\frac{\Psi_a}{\bar{s}} \frac{1}{Z_{c,a} Z_{L,a} + Z_{c,a} \tanh \Gamma_a} \frac{Z_{c,a} + Z_{L,a} \tanh \Gamma_a}{Z_{c,a} Z_{L,a} + Z_{c,a} \tanh \Gamma_a}$$

$$\frac{\bar{\Phi}_b}{\bar{T}_b}(\bar{s}) = \Psi_t h_t(\bar{s}) = -\frac{\Psi_t}{\bar{s}} \frac{1}{Z_{c,t} Z_{L,t} + Z_{c,t} \tanh \Gamma_t} \frac{Z_{c,t} + Z_{L,t} \tanh \Gamma_t}{Z_{c,t} Z_{L,t} + Z_{c,t} \tanh \Gamma_t}$$

Graphical results of modelling the above transfer functions are obtained via software solutions described in (Aarsnes and Aamo, 2016) and shown in figure 3.

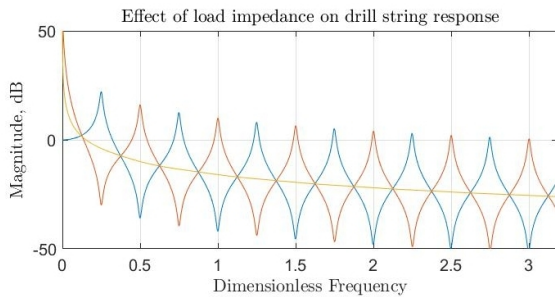
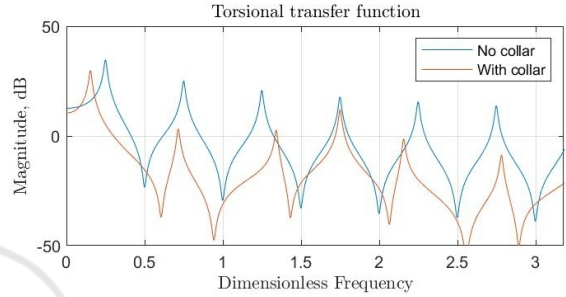


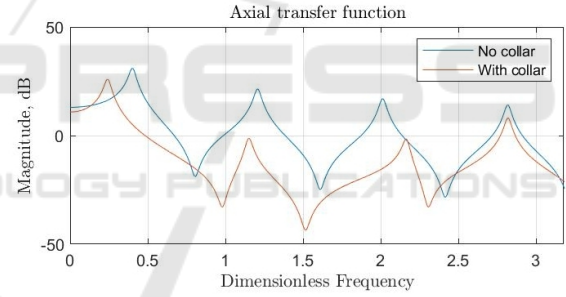
Figure 3: Drill collar sensors.

The bottom section of the drill string usually consists of weighted drill collars, which can have a great impact on dynamics of the drill string due to their extra inertia. In particular, transition from collars to couplings in the drill string causes reflections in traveling waves due to a change in the characteristic impedance of the line.

The length of sections is included in propagation operators, so they determine basic frequencies of an individual section. Figure 4 demonstrates the impact of a 200m drill collar on a 1200m drill string on transfer functions.



(a)



(b)

Figure 4: Transfer function with and without drill collars: a – torsional, b – axial.

To determine the rotary speed, we calculate the centripetal acceleration $A_c(t)$ (Cobern, 2003):

$$A_c(t) = (A_1(t) + A_2(t) + A_3(t))/3 \quad (3)$$

As $A_c(t) = \omega^2(t) \cdot r$, where r is the sensor radius, ω is the angular rotary speed, radian/sec. From here:

$$\omega(t) = \sqrt{\frac{A_c(t)}{r}} \quad (4)$$

the instantaneous speed is determined by the expression:

$$RPM = \left(\frac{60}{2\pi}\right) \cdot \omega(t) \quad (5)$$

The stick-slip effect is set by the maximum rotary speed (Cobern, 2003):

$$\omega_{ss} = \max(\omega(t)) \quad (6)$$

The reverse precession is determined by the peak of the following expression (Cobern, 2003):

$$A_w(t) = A_1(t) + A_2(t) \cos(120 \text{ deg}) + A_3(t) \cos(240 \text{ deg})$$

Lateral vibration has two components. The x-axis acceleration is equal to:

$$A_x(t) = \frac{1}{2} \left(\frac{A_2(t) - A_c(t)}{\cos(30)} - \frac{A_3(t) - A_c(t)}{\cos(30)} \right) \quad (7)$$

The y-axis acceleration is determined by the formula:

$$A_y(t) = \frac{1}{3} (A_1(t) - A_c(t) + \frac{-A_2(t) + A_c(t)}{\sin(30)} - \frac{-A_3(t) + A_c(t)}{\sin(30)})$$

Thus, the value of lateral vibration is determined by the vector sum (Cobern, 2003):

$$A_{Lat}(t) = \sqrt{A_x(t)^2 + A_y(t)^2} \quad (8)$$

Axial vibration can be directly measured with an axial accelerometer.

To verify the mathematical model, the data on drill string operation published in (Tunkiel et al., 2021) is used. On figure 5 shows the results of measuring the weight-on-bit depending on the depth of the borehole.

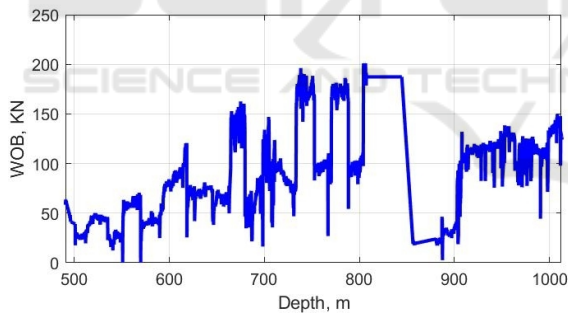
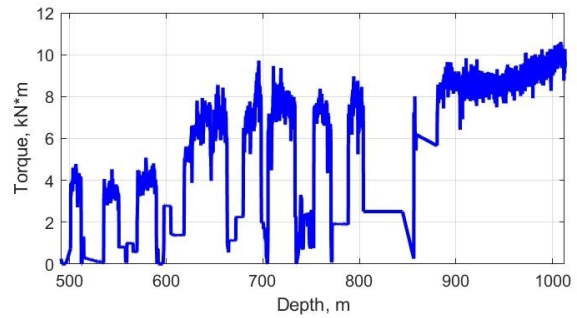


Figure 5: Dependence of the weight-on-bit on the borehole depth.

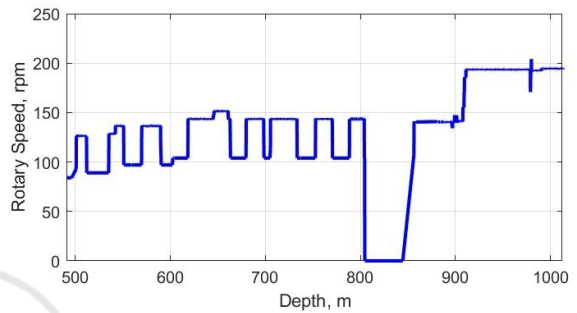
The graph of a dependence of the weight-on-bit on the borehole depth demonstrates characteristic stick-slip changes in the weight indicator which may be associated with alternation of various types of drilled rocks. On figure 6 revealed a dependence of the torque and the rotary speed on the borehole depth. These dependences are also characterized by areas with a stick-slip change in the indicator as in the case with the WOB indicator.

On figure 7 it is shown the change of the resulting indicator value (the ROP of the borehole) depending on the depth.

When studying the data on the drilling process, the above parameters are used as input variables: WOB,



(a)



(b)

Figure 6: Dependence of the torque and the rotary speed on the borehole depth: a – torque, b – rotary speed.

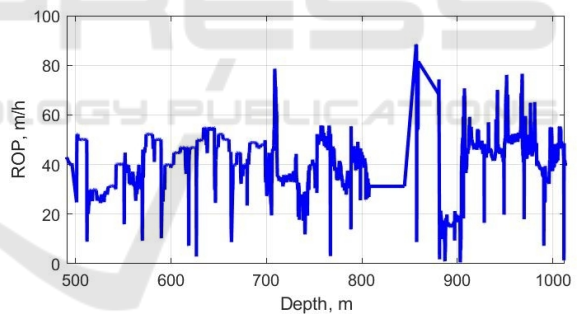


Figure 7: Drilling parameters.

RPM, torque, MSE, longitudinal, transverse and torsional vibrations. The resulting variable in this study is the ROP of the borehole.

Considering the above parameters, a mathematical model of the drilling process is formed on the basis of adaptive neural-fuzzy inference structures (ANFIS). There are three input terms of membership functions. The type of input membership functions is bell-shaped. On figure 8 it is shown the results of verification of the resulted model.

The verification results of the developed model on the test sample (figure 8) confirm its applicability to practical use. The accuracy of this model is 95.56 %.

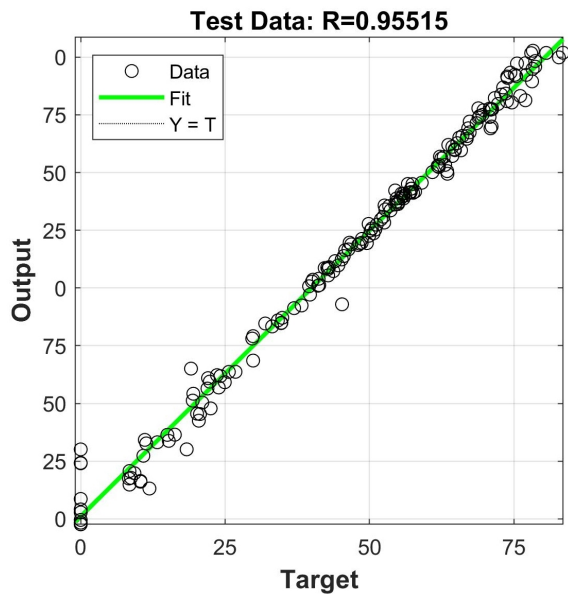


Figure 8: Modelling results.

4 CONCLUSIONS

To reduce negative impacts of vibrations occurring in the drill string at deep drilling of hard rocks, a mathematical model is proposed to consider parameters of the drilling process and predict the penetration rate. When studying the data on the drilling process, the above parameters are used as input variables: WOB, RPM, torque, MSE, longitudinal, transverse and torsional vibrations. The resulting variable is the ROP of the borehole. Considering the above parameters, a mathematical model of the drilling process is formed on the basis of adaptive neural-fuzzy inference structures (ANFIS). The accuracy of the given model makes 95.56 %.

REFERENCES

- Aarsnes, U. J. F. and Aamo, O. M. (2016). Linear stability analysis of self-excited vibrations in drilling using an infinite dimensional model. *Journal of Sound and Vibration*, 360:239–259. <https://doi.org/10.1016/j.jsv.2015.09.017>.
- Bogomolov, R. M. and Serikov, D. Y. (2018). Vibration damper-calibrator. *Equipment and Technologies for Oil and Gas Complex*, 3:39–43. <https://doi.org/10.30713/1999-6934-2018-3-39-43>.
- Coburn, M. E. (2003). Downhole vibration monitoring & control system. Final report, APS Technology. <https://doi.org/10.2172/831129>.
- Deng, P., Zhang, A., Fu, K., and Li, H. (2021). Nonlinear Vibration of a Time-Space Coupled Drill String System Based on the Surface Morphology of Rock. *Journal of Sound and Vibration*, 506:116153. <https://doi.org/10.1016/j.jsv.2021.116153>.
- Golik, V., Komashchenko, V., Morkun, V., and Zaalishvili, V. (2015). Enhancement of lost ore production efficiency by usage of canopies. *Metallurgical and Mining Industry*, 7(4):325–329. https://www.metaljournal.com.ua/assets/MMI_2014_6/MMI_2015_4/047-GolikKomashchenkoMorkunZaalishvili.pdf.
- Liu, Y., Li, Q., Qi, Z., and Chen, W. (2021). Defect suppression mechanism and experimental study on longitudinal torsional coupled rotary ultrasonic assisted drilling of CFRPs. *Journal of Manufacturing Processes*, 70:177–192. <https://doi.org/10.1016/j.jmapro.2021.08.042>.
- Moharrami, M. J., de Arruda Martins, C., and Shiri, H. (2021). Nonlinear integrated dynamic analysis of drill strings under stick-slip vibration. *Applied Ocean Research*, 108:102521. <https://doi.org/10.1016/j.apor.2020.102521>.
- Morkun, V., Morkun, N., and Pikilnyak, A. (2014). Modeling of ultrasonic waves propagation in inhomogeneous medium using fibered spaces method (k-space). *Metallurgical and Mining Industry*, 6(2):43–48. <https://www.metaljournal.com.ua/assets/Journal/a8.pdf>.
- Morkun, V., Morkun, N., and Tron, V. (2015a). Distributed control of ore beneficiation interrelated processes under parametric uncertainty. *Metallurgical and Mining Industry*, 7(8):18–21. https://www.metaljournal.com.ua/assets/Journal/english-edition/MMI_2015_8/004Morkun.pdf.
- Morkun, V., Morkun, N., and Tron, V. (2015b). Identification of control systems for ore-processing industry aggregates based on nonparametric kernel estimators. *Metallurgical and Mining Industry*, 7(1):14–17. https://www.metaljournal.com.ua/assets/Journal/english-edition/MMI_2015_1/3%20Morkun,%20Tron.pdf.
- Morkun, V., Morkun, N., and Tron, V. (2015c). Model synthesis of nonlinear nonstationary dynamical systems in concentrating production using Volterra kernel transformation. *Metallurgical and Mining Industry*, 7(10):6–9. https://www.metaljournal.com.ua/assets/Journal/english-edition/MMI_2015_10/001Morkun.pdf.
- Morkun, V. and Tron, V. (2014). Automation of iron ore raw materials beneficiation with the operational recognition of its varieties in process streams. *Metallurgical and Mining Industry*, 6(6):4–7. https://www.metaljournal.com.ua/assets/MMI_2014_6/1-MorkunTron.pdf.
- Novikov, A. S. and Serikov, D. Y. (2020). Some features of the work of drill bits and practical techniques for their use [Nekotorye osobennosti raboty burovkykh dolot i prakticheskie priemy pri ikh ispolzovanii]. *Sphere. Oil and Gas*, 2:44–49. https://xn--80aaiqbog2bzaiqsf7i.xn--p1ai/upload/journal/sphereoilandgas_2020-2.pdf.
- Serikov, D. Y. and Ginzburg, E. S. (2015). Increasing the efficiency of destruction of medium and hard rocks

- through the use of helical cones [Povyshenie effektivnosti razrusheniia srednikh i tverdykh porod putem ispolzovaniia kosozubogo vooruzheniia sharoshek]. *Equipment and Technologies for Oil and Gas Complex*, 4:18–22. <https://www.elibrary.ru/item.asp?id=23868184>.
- Serikov, D. Y., Panin, N. M., and Ageeva, V. N. (2016). Improvement of sealing systems for bearing assemblies of cone bits [Sovershenstvovanie sistem germetizatsii podshipnikovykh uzlov sharoshechnykh dolot]. *Construction of oil and gas wells on land and at sea*, 4:16–19. <https://www.elibrary.ru/item.asp?id=25849083>.
- Sharma, A., Al Dushaishi, M., and Nygaard, R. (2021). Fixed Bit Rotary Drilling Failure Criteria Effect on Drilling Vibration. In *U.S. Rock Mechanics/Geomechanics Symposium*, volume All Days, page 116–121. <https://onepetro.org/ARMAUSRMS/proceedings-pdf/ARMA21/All-ARMA21/ARMA-2021-2083/2480289/arma-2021-2083.pdf>.
- Tunkiel, A. T., Sui, D., and Wiktorski, T. (2021). Reference dataset for rate of penetration benchmarking. *Journal of Petroleum Science and Engineering*, 196:108069. <https://doi.org/10.1016/j.petrol.2020.108069>.
- Vasiliev, A. A., Vyshegorodtseva, G. I., and Serikov, D. Y. (2015). Study of the influence of the flushing scheme of a roller-cone drill bit on the bottom hole cleaning [Issledovanie vliianiia skhemy promyvki sharoshechnogo burovogo dolota na ochildku zaboia skvazhiny]. *Construction of oil and gas wells on land and at sea*, 5:25–28. <https://www.elibrary.ru/item.asp?id=23702308>.

